

# Quantitative analysis on correlation between local coercivity and reversal time in ferromagnetic thin films

Sug-Bong Choe<sup>a)</sup> and Sung-Chul Shin

*Department of Physics and Center for Nanospinics of Spintronic Materials, Korea Advanced Institute of Science and Technology, Taejeon 305-701, Korea*

(Received 28 January 2000; accepted for publication 15 June 2000)

We report a method to quantitatively analyze the correlation between the local coercivity variation and the local reversal-time distribution in ferromagnetic thin films. The spatial distribution of the local coercivity on a film plane was directly measured from the hysteresis loops of each local area of  $320 \times 320 \text{ nm}^2$  and then, the local coercivity distribution was quantitatively correlated with the local reversal-time distribution obtained from time-resolved domain evolution patterns grabbed at precisely the same position of the film. We demonstrate a clear experimental evidence of the direct correlation between the real coercivity distribution and the magnetization reversal dynamics, which could be explained within a context of a thermally activated relaxation process. © 2000 American Institute of Physics. [S0021-8979(00)07718-5]

Magnetization reversal dynamics in ferromagnetic thin films is of current fundamental interest in achieving high performance of technological applications as well as in exploring fundamental curiosity in magnetism.<sup>1-4</sup> Recently, advanced magnetic imaging techniques provide direct observation of domain evolution patterns and promptly, the experimental observations of the ragged domain boundaries evidence the existence of the local magnetic irregularities and their influence on the domain reversal dynamics.<sup>5-7</sup>

Much effort has been devoted to clarify the influence of the local magnetic irregularities on the domain reversal dynamics.<sup>7-14</sup> For instance, Bruno *et al.*<sup>9</sup> took into account the distribution of activation energies to explain the hysteresis loop and the distortion in wall displacement of ferromagnetic Au/Co/Au film. Ferré *et al.*<sup>7,8</sup> introduced the local coercivity field distribution into a micromagnetic consideration to analyze the direct/indirect magnetization processes and the “Swiss cheese”-shaped domain patterns. However, to the best of our knowledge, all the previous investigations have been done based on the models of the coercivity distribution and thus, actual correlation still remains open. The present work was motivated to directly measure the distribution of the local coercivity to quantitatively analyze the influence of the local coercivity variation on the domain reversal dynamics. This letter first demonstrates the experimental evidence that the reversal time of each local area in ferromagnetic thin films is directly determined by its local coercivity.

In this work, the spatial distribution of the local coercivity has been measured from each local hysteresis loop of local area on two-dimensional array of  $320 \times 320 \text{ nm}^2$  spots on a ferromagnetic film.<sup>8,15,16</sup> The local coercivity distribution was directly analyzed with the local reversal-time distribution at precisely the same position of the film obtained from time-resolved domain evolution patterns grabbed in

real time by a magneto-optical microscope magnetometer (MOMM) system.<sup>3</sup>

A number of Co/Pd multilayers were prepared on glass substrates by alternatively exposing two e-beam sources of Co and Pd under a base pressure of  $2.0 \times 10^{-7}$  Torr at the ambient temperature. The layer thickness was carefully controlled within a 4% accuracy. Low-angle x-ray diffraction studies using Cu  $K\alpha$  radiation revealed that all samples had distinct peaks indicating an existence of the multilayer structure. High-angle x-ray diffraction studies showed that the samples grew along the [111] cubic orientation. All the samples have perpendicular magnetic anisotropy and show hysteresis loops of unit squareness. We will designate the samples as  $(t_{\text{Co}}\text{-}\text{\AA}\text{Co}/t_{\text{Pd}}\text{-}\text{\AA}\text{Pd})_n$ , where  $t_{\text{Co}}$  is the Co-sublayer thickness,  $t_{\text{Pd}}$  is the Pd-sublayer thickness, and  $n$  is the number of repeats.

The hysteresis loops of every local area from two-dimensional array of 8000 spots on the Co/Pd multilayers were simultaneously measured utilizing the MOMM system.<sup>15</sup> The system, mainly composed of an optical polarizing microscope equipped with a charge-coupled device (CCD) camera, could grab domain images with 300 nm spatial resolution with sweeping the external magnetic field by an electromagnet.<sup>3</sup> The local Kerr hysteresis loops were measured by simultaneously tracing the Kerr intensity variation at every corresponding CCD pixel for every 10 Oe interval per 0.4 s and then, converting the Kerr intensity to the Kerr rotational angle.<sup>8,15,16</sup> The Kerr intensity was averaged by 16-times measurements of the major loops for a given sample to reduce the error from the statistical reversal probability. Care was taken to maintain the observation sight of the MOMM measurement preventing the thermal and/or gravitational drift and the mechanical vibration of the sample stage during the measurement. The coercivity  $H_C$  was determined by interpolating an applied field for the condition of zero Kerr rotational angle. The experimental error in the coercivity determination was confirmed to be smaller than 2 Oe

<sup>a)</sup>Electronic mail: sugbong@kaist.ac.kr

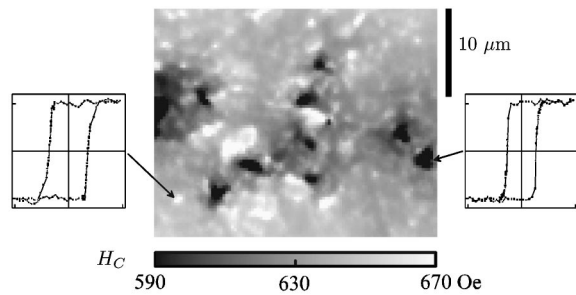


FIG. 1. The local coercivity distributions  $H_C(x,y)$  of the  $(2.5 \text{ \AA} \text{ Co}/11 \text{ \AA} \text{ Pd})_{10}$  sample. The plots show the hysteresis loops measured at the unit pixels corresponding to two local areas designated by each arrow. Here,  $x$  axis is an applied field ranging from  $-2$  to  $2$  kOe and  $y$  axis is the normalized Kerr rotational angle.

for these particular Co/Pd multilayers having the maximum Kerr rotational angle of about  $0.15^\circ$ .

The most striking feature of the MOMEM system is the fact that we can generate the two-dimensional spatial distribution map of the local coercivity variation of a sample, from directly analyzing the local hysteresis loops of every local area simultaneously measured with an identical condition. Figure 1 demonstrates the local coercivity distribution  $H_C(x,y)$  of the  $(2.5 \text{ \AA} \text{ Co}/11 \text{ \AA} \text{ Pd})_{10}$  sample in gray level onto the two-dimensional  $xy$  plane, where each map corresponds to a sample surface area of  $32.0 \times 25.6 \mu\text{m}^2$  and each pixel corresponds to an area of  $320 \times 320 \text{ nm}^2$ . The figure vividly shows the spatial fluctuation of the local coercivity on submicrometer scale. The difference in the loop shape and the coercivity is clearly seen between the plots in the left and right side of the figures, which show the hysteresis loops measured at the unit pixels corresponding to two different local spots designated by each arrow. The fluctuation of the local coercivity is possibly ascribed to the structural irregularity due to the possible accumulation of the lattice misfits, residual stress, and other defects, especially at the interfaces during deposition process in high vacuum, since the coercivity is a structure-sensitive magnetic property.<sup>17</sup> Therefore, one might expect a larger variation in the local coercivity with increasing the number of repeats; it was indeed observed in our Co/Pd multilayer samples.<sup>15</sup>

In Fig. 2 we plot the distribution density of the local

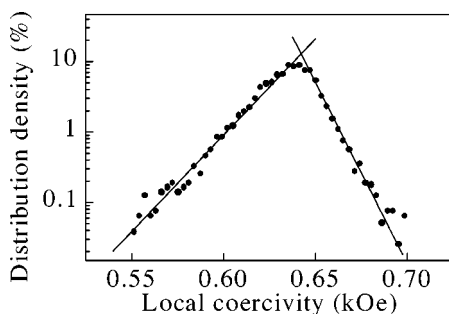


FIG. 2. The distribution density in magnitude of the local coercivity of the  $(2.5 \text{ \AA} \text{ Co}/11 \text{ \AA} \text{ Pd})_{10}$  sample. The density was determined by counting the number of cells having the corresponding magnitude of the local coercivity for every 3 Oe interval. The solid lines are the best fits for the linear dependency of each bound.

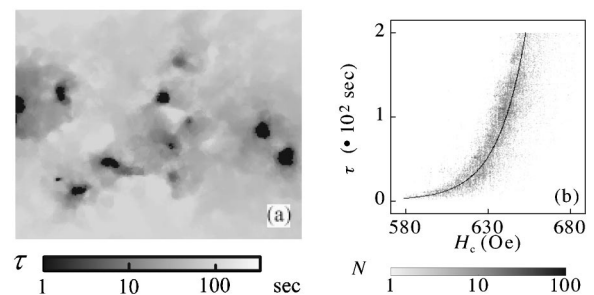


FIG. 3. (a) The time-resolved domain reversal pattern of the  $(2.5 \text{ \AA} \text{ Co}/11 \text{ \AA} \text{ Pd})_{10}$  sample at exactly the same position shown in Fig. 1. The gray level corresponds to the time  $\tau(x,y)$  in a logarithmic scale for reversal of the corresponding region  $(x,y)$ . (b) The correlated distribution of the number of pixels  $N(H_C, \tau)$  with logarithmic gray level in  $H_C - \tau$  coordinate for the  $(2.5 \text{ \AA} \text{ Co}/11 \text{ \AA} \text{ Pd})_{10}$  sample. The solid line represents the best fit using Eq. (1).

coercivity of this sample, by counting the cells having the corresponding value of the local coercivity for every 3 Oe interval. Here, the distribution density is normalized by the total number of 8000 cells. The asymmetric shape might be ascribed to the difference between the wall-pinning and nucleation energy barrier distributions, where the lower bound of the coercivity distribution is governed by the wall-pinning coercivity and the upper bound is determined by the nucleation coercivity.<sup>18</sup> It should be noticed that the distribution in magnitude is neither a Gaussian nor a Lorentzian as generally assumed in the most theoretical models.<sup>7,9</sup> Surprisingly, the distribution of our samples could be well fitted by the linear lines in exponential scale as shown by the solid lines in the figure.

It is very interesting to directly correlate the real distribution of the local coercivity with the magnetization reversal dynamics. For this study, we have investigated the magnetization reversal dynamics of the Co/Pd multilayers at *precisely the same* position as the local coercivity measurement of the sample. It was done via the time-resolved domain observation utilizing the MOMEM system by applying a constant reversing magnetic field near the average coercivity after saturating the sample.<sup>3</sup> Figure 3(a) shows the domain evolution patterns for the  $(2.5 \text{ \AA} \text{ Co}/11 \text{ \AA} \text{ Pd})_{10}$  sample, where the gray level in the figure designates the time  $\tau(x,y)$  required for the corresponding region of the  $(x,y)$ th pixel to reverse. Most interestingly, one can notice that the reversal pattern in Fig. 3(a) is truly coincident with the local coercivity distribution in Fig. 1. This directly demonstrates the close correlation between the local coercivity distribution and domain reversal pattern on the submicron scale.

For a quantitative analysis of the correlation, we have measured the number of pixels  $N(H_C, \tau)$  by counting the pixels having the values of the local coercivity  $H_C(x,y)$  and the local reversal time  $\tau(x,y)$  at the same  $(x,y)$ th pixel in the corresponding map. Figure 3(b) illustrates the correlated distribution of the number of pixels  $N(H_C, \tau)$  in logarithmic scale in  $H_C - \tau$  coordinates. In the figure, it is very clearly seen that the local reversal time is truly correlated with the local coercivity, which implies that the local domain dynam-

ics during magnetization reversal is directly governed by the local coercivity.

The reversal mechanism taking into account the local coercivity distribution could be analyzed within the context of a thermally activated relaxation process. The half reversal time  $\tau$ , the time needed to reverse half the volume of the sample, is known to be exponentially dependent on an applied field  $H$ .<sup>4</sup> By considering the local coercivity distribution  $H_C(x,y)$ , the half reversal time  $\tau(x,y)$  of the magnetization  $M_S$  of a volume  $V_A$  located at  $(x,y)$  is given by

$$\tau(x,y) = \tau_0 \exp\left(\frac{V_A M_A}{k_B T} [H_C(x,y) - H]\right), \quad (1)$$

where  $\tau_0$  is the characteristic reversal time for  $H = H_C(x,y)$ ,  $k_B$  is the Boltzmann's constant, and  $T$  is temperature.<sup>4</sup> It is clearly demonstrated that the correlated distribution can be quantitatively characterized by Eq. (1) as shown by the solid line in Fig. 3(b). The activation volume  $V_A$  of the sample is determined to be  $7.9 \times 10^{-18}$  cc, which is almost identical to the previous value determined via the field dependence of the half reversal time in the whole area of the sample.<sup>19</sup>

In conclusion, we have developed a novel method to directly measure the spatial distribution of the local coercivity by simultaneously measuring a two-dimensional array of hysteresis loops at each pixel of  $320 \times 320$  nm<sup>2</sup> utilizing a magneto-optical microscope magnetometer (MOMM). The local coercivity distribution of Co/Pd multilayered samples has been investigated and interestingly, the coercivity of the samples was found to be spatially nonuniform on submicrometer scale. The local coercivity distribution is directly analyzed with the domain reversal patterns grabbed at *precisely the same* position, and it is clearly demonstrated that

the local coercivity distribution governs the domain reversal dynamics via a thermally activated relaxation process.

This work was supported by the Creative Research Initiatives of the Ministry of Science and Technology of Korea.

- <sup>1</sup>J. Ferré, J. P. Jamet, and P. Meyer, Phys. Status Solidi A **175**, 213 (1999).
- <sup>2</sup>B. Raquet, R. Mamy, and J. C. Ousset, Phys. Rev. B **54**, 4128 (1996).
- <sup>3</sup>S.-B. Choe and S.-C. Shin, Phys. Rev. B **57**, 1085 (1998); Appl. Phys. Lett. **70**, 3612 (1997).
- <sup>4</sup>J. Pommier, P. Meyer, G. Pónissard, J. Ferré, P. Bruno, and D. Renard, Phys. Rev. Lett. **65**, 2054 (1990).
- <sup>5</sup>B. E. Bernacki, T.-H. Wu, and M. Mansuripur, J. Appl. Phys. **73**, 6838 (1993).
- <sup>6</sup>M. Speckmann, H. P. Oepen, and H. Ibach, Phys. Rev. Lett. **75**, 2035 (1995).
- <sup>7</sup>J. Ferré, V. Grolier, P. Meyer, S. Lemerle, A. Maziewski, E. Stefanowicz, S. V. Tarasenko, V. V. Tarasenko, and M. Kisielewski, Phys. Rev. B **55**, 15092 (1997).
- <sup>8</sup>J.-P. Jamet, S. Lemerle, P. Meyer, J. Ferré, B. Bartenlian, N. Bardou, C. Chappert, P. Veiller, F. Rousseaux, D. Decanini, and H. Launois, Phys. Rev. B **57**, 14320 (1998).
- <sup>9</sup>P. Bruno, G. Bayreuther, P. Beauvillian, C. Chapert, G. Lugert, D. Renard, J. P. Renard, and J. Seiden, J. Appl. Phys. **68**, 5759 (1990).
- <sup>10</sup>S. K. Han, S.-C. Yu, and K. V. Rao, J. Appl. Phys. **79**, 4260 (1996).
- <sup>11</sup>A. Moschel, R. A. Hyman, and A. Zangwill, Phys. Rev. Lett. **77**, 3653 (1996).
- <sup>12</sup>P. Cizeau, S. Zapperi, G. Durin, and H. E. Stanley, Phys. Rev. Lett. **79**, 4669 (1997).
- <sup>13</sup>H. Jaffèrès, L. Ressier, J. P. Peyrade, A. R. Fert, P. Gogol, A. Thiaville, A. Schuhl, and F. N. V. Dau, J. Appl. Phys. **84**, 4375 (1998).
- <sup>14</sup>P. Haibach, M. Huth, and H. Adrian, Phys. Rev. Lett. **84**, 1312 (2000).
- <sup>15</sup>S.-B. Choe, H.-J. Jang, and S.-C. Shin, J. Appl. Phys. **87**, 6848 (2000).
- <sup>16</sup>T. Aign, P. Meyer, S. Lemerle, J. P. Jamet, J. Ferré, V. Mathet, C. Chappert, J. Gierak, C. Vieu, F. Rousseaux, H. Launois, and H. Bernas, Phys. Rev. Lett. **81**, 5656 (1998).
- <sup>17</sup>H. Kronmüller, Phys. Status Solidi B **144**, 385 (1987).
- <sup>18</sup>T. Thomson and K. O'Grady, J. Phys. D **30**, 1566 (1997).
- <sup>19</sup>S.-B. Choe and S.-C. Shin, J. Appl. Phys. **87**, 5076 (2000).